Developing Diagnostic Tools for Low-Burnup Reactor Samples

Patrick Jaffke, Benjamin Byerly, Jamie Doyle, Anna Hayes, Gerard Jungman, Steven Myers, Angela Olson, Donivan Porterfield, and Lav Tandon

Phys. Rev. Applied **8**, 044025 — Published 31 October 2017

DOI: 10.1103/PhysRevApplied.8.044025

Developing diagnostic tools for low-burnup reactor samples

Patrick Jaffke,[1,*] Benjamin Byerly,[1,2] Jamie Doyle,[1] Anna Hayes,[1] Gerard Jungman,[1] Steven Myers,[1] Angela Olson,[1] Donivan Porterfield,[1] and Lav Tandon[1]

[1] *Los Alamos National Laboratory, Los Alamos, NM 87545, USA*
[2] *Department of Geology and Geophysics, Louisiana State University, Baton Rouge, LA 70803, USA*

(Dated: October 6, 2017)

We test common neutron fluence diagnostics in the very low burnup regime for natural uranium reactor samples. The fluence diagnostics considered are the uranium isotopics ratios $^{235}U/^{238}U$ and $^{236}U/^{235}U$, for which we find simple analytic formulas agree well with full reactor simulation predictions. Both ratios agree reasonably well with one another for fluences in the mid 10^{19} n/cm^2 range. However, below about 10^{19} n/cm^2 the concentrations of ^{236}U are found to be sufficiently low that the measured $^{236}U/^{235}U$ ratios become unreliable. We also derive and test diagnostics to determine the cooling times in situations where very low burnup and very long cooling times render many standard diagnostics, such as the $^{241}Am/^{241}Pu$ ratio, impractical. We find that using several fragment ratios are necessary to detect the presence of systematic errors, such as fractionation.

I. ISOTOPICS INTRODUCTION

Determining the reactor environment that a particular spent fuel sample experienced is critical information for nonproliferation and reactor verification. In particular, the neutron fluence (or exposure) is often related to the fuel burnup and, hence, the plutonium production and grade [1]. This makes the fluence an important parameter for nonproliferation and arms reduction [2]. The fluence of a sample can be inferred in many ways, but is most commonly derived from isotopic ratios of actinides, such as $^{235}U/^{238}U$ or $^{236}U/^{235}U$ [3, 4] and various plutonium ratios [5]. Additional methods utilize the ratios of activated isotopes in cladding and moderator material, such as the graphite isotope ratio method (GIRM) [6–8], or of ratios of long-lived fragments such as cesium [5, 9, 10], europium [9], or neodymium [5]. The cooling time is often determined with ratios utilizing short-lived actinides, such as $^{241}Pu/^{241}Am$ [11], but can also be inferred by gamma spectroscopy of fragments [12]. The cooling time provides one with an estimate of the sample age, which is also pertinent for forensics and nonproliferation.

One can determine the final activities, abundances, and ratios of nuclides with detailed reactor simulations, provided a burnup history and initial fuel composition. Our goal is to invert this process, where one begins with measured isotopic abundances or ratios and then determines the reactor parameters. In particular, we focus on the neutron fluence Φ defined as the time integral of the neutron flux $\phi(t)$, or $\Phi = \int \phi(t)dt$, and the total cooling time T_c defined as the sum of all non-irradiation time. These two parameters can be derived from so-called linear systems, which have simpler analytical forms, in the low burnup regime. Non-linear systems can be used to infer parameters, such as the flux and shutdown history [13]. We used low burnup archived samples, available at Los Alamos National Laboratory. The chemical analyses to determine the abundances of the actinides and fission fragments for our low burnup samples can be found in Ref. [14] and Ref. [15]. The declared irradiation times of our samples were 85 hr or less with thermal fluxes ranging from $10^{13} - 10^{14}$ n/cm^2/sec. In this very low burnup regime, new cooling time diagnostics must be developed. They are verified alongside the standard fluence diagnostics. Several cooling time diagnostics are utilized to detect the presence of systematic errors.

This paper is structured as follows. The fluence diagnostics are discussed in Sec. II. Cooling time diagnostics are discussed and derived in Sec. III. The diagnostics are verified with reactor simulations and theoretical errors are generated in Sec. IV. The diagnostics are then applied to low burnup reactor samples to determine their fluence, cooling time, and sensitivity to systematic errors in Sec. V. We conclude in Sec. VI.

II. FLUENCE DIAGNOSTICS

The fluence diagnostics considered in this work utilize the uranium isotopic ratios: $^{235}U/^{238}U$ and $^{236}U/^{235}U$. Ratios utilizing moderator materials cannot be used as they require a sample removal from the existing reactor, which may not be feasible and impacts future reactor design and safety. In addition, some commonly used long-lived fragments, such as ^{134}Cs or ^{154}Eu, are not produced in sufficient quantities in these very low burnup scenarios and create experimental difficulties. Finally, ^{239}Pu cannot be used, as its accumulation is not precisely linear in fluence at low burnup and, thus, displays a flux dependence. For these reasons, we focus on the uranium ratios above which are trivially related to the fluence via

$$\begin{aligned}\epsilon(\Phi, \epsilon_0) &= \epsilon_0 e^{-\Phi(\sigma^T_{U235} - \sigma^T_{U238})} \\ \rho(\Phi) &= \left(\frac{\sigma^c_{U235}}{\sigma^T_{U236} - \sigma^T_{U235}}\right)\left(1 - e^{-\Phi(\sigma^T_{U236} - \sigma^T_{U235})}\right).\end{aligned} \tag{1}$$

* corresponding author: pjaffke@lanl.gov

Here, ϵ denotes the ^{235}U/^{238}U ratio and ρ the ^{236}U/^{235}U ratio, where ϵ_0 is the initial fuel ratio. The superscripts on the cross-sections σ are for capture (c) or total (T) reactions and we use a one-group fluence for brevity.

As ϵ depends on the initial ratio ϵ_0, a measurement of Φ via the ^{235}U/^{238}U ratio is only valid when the initial enrichment is known. In the case of our low burnup samples, all indicated natural uranium (NU) as the initial fuel [14]. On the other hand, the determination of Φ from ρ is insensitive to the initial fuel, but requires a measurement of ^{236}U, which is produced in very low quantities when the burnup is low. A final note is that a measurement of Φ using Eq. 1 will be most sensitive to the thermal fluence, as these cross-sections dominate (specifically ^{235}U thermal fission).

Inverting Eq. 1 produces the fluence diagnostics we will apply to the low burnup samples

$$\begin{aligned}\Phi &= \frac{\ln(\epsilon_0/\epsilon)}{\sigma^T_{U235} - \sigma^T_{U238}} \\ \Phi &= \frac{1}{\sigma^T_{U235} - \sigma^T_{U236}} \ln\left(\frac{\sigma^c_{U235} - \rho(\sigma^T_{U236} - \sigma^T_{U235})}{\sigma^c_{U235}}\right).\end{aligned} \tag{2}$$

Measurement of the values of ϵ or ρ are typically accomplished by chemical separation [16–18], followed by gamma spectroscopy [5], thermal ionization mass spectrometry (TIMS) [14], or inductively coupled plasma mass spectrometry (ICP-MS) [3, 4]. Specifically, the measurement of ^{236}U is made difficult as isobaric interferences arise when small quantities of ^{236}U exist amidst large ^{235}U and ^{238}U quantities. Additionally, the α-decay peak of ^{235}U can interfere in a ^{236}U/^{238}U measurement done via α-spectrometry [19, 20].

III. COOLING TIME DIAGNOSTICS

Cooling time diagnostics must be selected specifically for the context of low burnup samples. For example, the ^{241}Pu/^{241}Am ratio cannot be used as neither ^{241}Pu nor ^{241}Am are produced in appreciable amounts at low burnups. Similar issues preclude the use of other unstable actinides from NU fuel or ^{134}Cs and ^{154}Eu, both of which are non-linear nuclides [21] that rely on neutron capture as their primary production channel. This indicates that common cooling time diagnostics that utilize same-species ratios to avoid fractionation [22], such as the ^{134}Cs/^{137}Cs ratio [23], are invalid. In addition, our samples exhibited extremely long cooling times ($\sim 20\,$yr), which we define as the sum of all decay periods including shutdowns, which invalidate the use of some major decay heat tags, such as ^{106}Ru and ^{144}Ce [24] as their halflife is too short. Thus, the cooling time diagnostic requires nuclides that are appreciably produced in low burnup scenarios, have long half-lives, and are easy to chemically separate and analyze. These requirements naturally lead one to the so-called 'linear' fission fragments, described by:

1. The linear fragment N_L has a halflife $t^L_{1/2}$ such that $\lambda_L T_{\rm irr} \ll 1$, with $\lambda_L = \ln(2)/t^L_{1/2}$.
2. The cumulative fission product yields for N_L, $\vec{Z}_L$, are large. $\vec{Z}_L = [Z^L_{U235}, Z^L_{U238}, Z^L_{Pu239}, Z^L_{Pu241}]$
3. The beta-parents of N_L have halflives such that they are in equilibrium during $T_{\rm irr}$.

These fragments are dubbed 'linear' as their production is linear in Φ, i.e. the number of fissions. The first criteria ensures that the fragment is long-lived relative to the irradiation period of the reactor. In our circumstances, where $T_{\rm irr}$ is very short compared to the suspected cooling time T_c, one should modify criteria 1 so that N_L does not completely decay during the cooling period (i.e. $\lambda_L(T_{\rm irr} + T_c) \ll 1$). The second criteria demands that the fragment is appreciably produced in fission. The third criteria allows one to derive a simple analytical expression for N_L, where the yields of the β-parents of N_L are accounted for by utilizing the cumulative fission yields of N_L. For our low burnup purposes, ^{85}Kr, ^{125}Sb, ^{137}Cs, and ^{155}Eu are linear fragments.

Nuclides in a reactor environment are governed by depletion equations, which form the basis for constructing an interaction matrix between the various nuclides. This structure is utilized by many reactor simulation codes [25, 26], which often solve these massive (~ 2000 species) systems as an eigenvalue problem [27]. In our case, we utilize linear fragments to construct a simple isolated system, which resembles a Bateman equation [28],

$$\frac{dN_L}{dt} = -\tilde{\lambda}_L N_L + \vec{Z}_L \cdot \vec{\mathcal{F}}. \tag{3}$$

The positive (negative) terms denote production (depletion) channels and we use an effective decay constant $\tilde{\lambda} = \lambda + \phi\sigma^T$. We note that the full depletion equation, which resembles Eq. 1 of Ref. [29], reduces to Eq. 3 after applying $\lambda_i \gg b_{j,i}\lambda_j$ (criteria 3), noting that $\sigma_{j,i}\phi \ll b_{j,i}\lambda_j$ is satisfied for most fragments except for particular reactions such as ^{135}Xe$(n,\gamma)^{136}$Xe, and adding an explicit fission term. Thus, Eq. 3 states that a linear fragment N_L is produced via fission at a rate $\vec{Z}_L \cdot \vec{\mathcal{F}} = \sum_f Z^f_L \mathcal{F}^f$, where f runs over the fissiles and $\mathcal{F}^f$ denotes a particular fissile's fission rate, and is depleted through its decay and neutron-capture.

Solving Eq. 3 yields

$$N_L(t) = \left(N_{L0} - \frac{\vec{Z}_L \cdot \vec{\mathcal{F}}}{\tilde{\lambda}_L}\right) e^{-\tilde{\lambda}_L t} + \frac{\vec{Z}_L \cdot \vec{\mathcal{F}}}{\tilde{\lambda}_L}, \tag{4}$$

with an initial nuclide abundance N_{L0}. Most linear fragments satisfy $\lambda_L \gg \phi\sigma^T_L$, but we include the neutron-capture channel in our derivations for completeness. One can easily verify that our selected fragments are linear

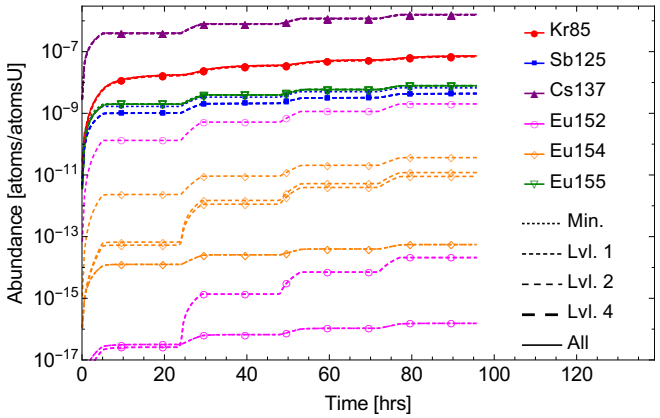

FIG. 1. Relative abundances of several fission fragments from a simulation of an irradiation history consisting of 4 [5, 19]hr ON/OFF periods and a thermal flux of $\phi_t = 8.5 \times 10^{13}\,\mathrm{n/cm^2/sec}$ beginning with natural uranium. The simulation uses CINDER08 [30] cross-sections and the decay data was allowed to vary between ENDF7 [31], JEFF [32], and JENDL [33], with no observed difference. Linear fragments show no dependence on the layer of nuclear data.

in nature using reactor simulations. We use a finite-difference methods solver for the interaction matrix, where the amount and source of nuclear data can be varied. A sample irradiation history is given by 4 cycles of [5, 19]hr ON/OFF periods and a thermal flux of $\phi_t = 8.5 \times 10^{13}\,\mathrm{n/cm^2/sec}$. The resulting relative abundances for our linear fragments and, for comparison, two non-linear fragments (^{152,154}Eu) are shown in Fig.1.

The minimum layer of nuclear data considered just our fragment of interest (FOI). This physically represents the case when each FOI is given by Eq. 4. Layer 1 added the β-parents and their fission yields. Layer 2 added the production via (n,γ) reactions and their yields. Layer 4 included the primary, secondary, and (in some cases) tertiary (n,γ) channels as well as all of their β-parents with halflives greater than 30 sec and yields. We also included a simulation of all nuclides with available data (~ 700). From Fig. 1, one can verify that ^{85}Kr, ^{125}Sb, ^{137}Cs, and ^{155}Eu are linear as they have very little dependence on the layer of nuclear data. Thus, the linear fragments can be analytically calculated via Eq. 4 using their halflives and cumulative fission yields instead of solving for each β-parent and using their halflife and direct fission yields. None of the fragments studied varied significantly between the major fission yields libraries [31–33].

To derive the cooling time diagnostic, we first expand Eq. 4 with $\tilde{\lambda} T_{\mathrm{irr}} \ll 1$ (criteria 1) and arrive at

$$N_L(t, T_c) = \Phi(\vec{Z}_L \cdot \vec{\Sigma}_{\mathrm{fiss}}) e^{-\lambda_L T_c} + \mathcal{O}((\tilde{\lambda}_L T_{\mathrm{irr}})^2). \quad (5)$$

Equation 5 assumes that $N_{L0} = 0$ and uses the relations $\Phi = \phi t$ and $\vec{\mathcal{F}} = \vec{\Sigma}_{\mathrm{fiss}} \phi$. As $\vec{\Sigma}_{\mathrm{fiss}}$ is the fission cross-sections weighted by the fissile abundances, one can determine $\vec{\Sigma}_{\mathrm{fiss}}$ with similar chemical analyses as those used for the fragments [14]. We also account for the decay of N_L after irradiation with the $e^{-\lambda_L T_c}$ term. The expansion to arrive at Eq. 5 is easily valid for all fragments used here, except ^{155}Eu which deviates from it by $\sim 1 - 3\%$ due to its large cross-section.

Universally setting $N_{L0} = 0$ appears to exclude cases with multiple irradiation cycles. Suppose we have a distribution of irradiation and cooling times described in Fig. 2, where t and τ are the total irradiation and cooling times across all cycles. We recursively insert Eq. 4

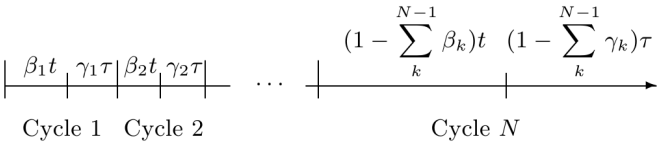

FIG. 2. Generalized irradiation history with N cycles, each consisting of an irradiation time of length $\beta_i t$ and cooling time $\gamma_i \tau$ with multiplicative factors β_i and γ_i that sum to unity. The N^{th} cycle is the remainder of the total irradiation time t and cooling time τ with time ascending from left to right.

into itself as an initial condition for the following irradiation and cooling period to verify that distributing the total irradiation and cooling time in a generalized way is a negligible effect on our linear fragments. We find that the final activity ($\alpha_L = \lambda_L N_L$) of a purely linear fragment (i.e. $\tilde{\lambda}_L = \lambda_L$) with a generic distribution of t and τ over N cycles is given by

$$\begin{aligned} \alpha_L(t, \tau, \vec{\beta}, \vec{\gamma}, N_{L0}) =& (\lambda_L N_{L0} - \vec{Z}_L \cdot \vec{\mathcal{F}}) e^{-\lambda_L (t+\tau)} \\ &+ (\vec{Z}_L \cdot \vec{\mathcal{F}}) e^{-\lambda_L \tau} \times f(\vec{\beta}, \vec{\gamma}), \end{aligned} \quad (6)$$

with a pre-irradiation initial abundance N_{L0} and the function $f(\vec{\beta}, \vec{\gamma})$ is given as a sum and product of exponentials over the additional $N - 1$ cycles

$$f(\vec{\beta}, \vec{\gamma}) = \left(\prod_{i=1}^{N-1} e^{\lambda_L \gamma_i \tau} \right) + e^{-\lambda_L t} \times$$
$$\sum_{i=1}^{N-1} \left[\left(\prod_{j=1}^{i} e^{\lambda_L \beta_j t} \right) \left(\prod_{k=1}^{i-1} e^{\lambda_L \gamma_k \tau} \right) - \left(\prod_{j=1}^{i} e^{\lambda_L (\beta_j t + \gamma_j \tau)} \right) \right]. \quad (7)$$

This complex function for N cycles reduces to unity when $N = 1$. One can show that criteria 1, and the fact that each β_i and γ_i are less than 1 by definition, restricts Eq. 7 to very small deviations from 1. We analyzed generic values for the β_i and γ_i within our expected t and τ ranges and found that Eq. 7 is well-constrained to $\lesssim 1\%$ deviations from unity. An exception to this is ^{125}Sb, which showed larger deviations when the decay time is concentrated towards earlier cycles (i.e. when $\gamma_1 \gg \gamma_{i \neq 1}$), but this is disfavored for our samples. Thus, with $f(\vec{\beta}, \vec{\gamma}) \approx 1$ for any reasonable choice of $\vec{\beta}$ and $\vec{\gamma}$, a single irradiation period of T_{irr} followed by a single cooling time of T_c is equivalent to the case of a series of ON/OFF cycles with total irradiation time T_{irr} and total cooling time, including intermediate shutdowns, T_c.

Now that we have justified our assumption of $N_{L0} = 0$, the final abundance of a linear fragment can be expressed as in Eq. 5. A ratio of the activities of two linear fragments removes the explicit dependence on Φ and creates the expression

$$\alpha_{n,d}(\vec{\Sigma}_{\text{fiss}}, T_c) = \frac{\lambda_n \vec{Z}_n \cdot \vec{\Sigma}_{\text{fiss}}}{\lambda_d \vec{Z}_d \cdot \vec{\Sigma}_{\text{fiss}}} e^{-(\lambda_n - \lambda_d)T_c}, \qquad (8)$$

which is a direct measure of the total cooling time. One can correct Eq. 8 with higher order terms to account for linear fragments with large neutron-capture components, but this will create a dependence on ϕ. For large fast fluences, one must replace $\vec{Z}_i \cdot \vec{\Sigma}_{\text{fiss}} \rightarrow \sum_g \Phi_g \times (\vec{Z}_i^g \cdot \vec{\Sigma}_{\text{fiss}}^g)$, to account for the different yields in fast fissions.

As mentioned previously, the final value of $\vec{\Sigma}_{\text{fiss}}$ is known from a measurement of fissile isotopics. However, $\vec{\Sigma}_{\text{fiss}}$ varies over the irradiation period. Therefore, one must average the weighted fission cross-sections so as not to bias Eq. 8 towards U or Pu fissions. The averaging is conducted linearly over the fluence Φ because neither T_{irr} nor ϕ are known. One can use the thermal fluence derived from Eq. 2 as the fluence endpoint and the initial value of $\vec{\Sigma}_{\text{fiss}}$ reflects natural uranium for our samples [14]. This fluence-averaged value $\langle \vec{\Sigma}_{\text{fiss}} \rangle_\Phi$ becomes a critical factor when predicting fragments that have cumulative yields that depend strongly on the fissioning nuclide.

Inverting Eq. 8 reveals the cooling time diagnostic

$$T_c = \frac{1}{\lambda_d - \lambda_n} \ln \left(\frac{\alpha_{n,d} \lambda_d \vec{Z}_d \cdot \langle \vec{\Sigma}_{\text{fiss}} \rangle_\Phi}{\lambda_n \vec{Z}_n \cdot \langle \vec{\Sigma}_{\text{fiss}} \rangle_\Phi} \right). \qquad (9)$$

Due to the pole in Eq. 9, two linear fragments with similar decay constants $\lambda_n \simeq \lambda_d$, such as a ratio of ^{90}Sr and ^{137}Cs, can produce large errors in the cooling time, but one can remove these numerically [34]. For fragments with large cross-sections, one can expand Eq. 4 to $\mathcal{O}((\tilde{\lambda} T_{\text{irr}})^2)$, but this introduces an unverifiable value for T_{irr} and only corrects the cooling time by a few percent.

IV. VERIFICATION

In Sec. II and Sec. III, we listed diagnostics for the thermal fluence and cooling time. These diagnostics were verified with the use of the reactor simulation described in Sec. III. Over 70 sample cases were evaluated with layer 4 nuclear data to determine the validity of the analytical calculations. The cases spanned a range of reasonable values for the thermal flux ϕ_t, cooling time T_c, fast flux ϕ_f, irradiation time T_{irr}, number of shutdowns N_s, and shutdown length T_s. The derived values for Φ and T_c, using Eq. 2 and Eq. 9, were compared with those used as input to the simulation. We found that the only parameter that affected the fluence diagnostic is the introduction of a fast flux ϕ_f as it slightly increases the final ρ and ϵ values, which could be mistaken for a larger thermal fluence. Using the maximum expected fast flux, the diagnostic of Eq. 2 returned the input fluence within $\sim 0.5\%$ for both the ^{235}U/^{238}U and ^{236}U/^{235}U ratios. The situation for the cooling time diagnostic was much more complicated.

We used the following ratios for the cooling time diagnostic: ^{137}Cs/^{155}Eu (α_1), ^{137}Cs/^{125}Sb (α_2), and ^{155}Eu/^{125}Sb (α_3). Diagnostics using ^{85}Kr were removed as it may have experienced volatile leakage. The derived cooling time was found to vary with all major reactor parameters listed above. As the total Φ_t increased, the errors on Eq. 9 increased linearly, but this was shown to be mediated somewhat by linearly averaging $\vec{\Sigma}_{\text{fiss}}$. The increase of ϕ_f created an underestimation of T_c proportional to the additional fast cumulative yields of the fragments used in Eq. 9. Increasing the cooling time served to decrease the errors on all T_c diagnostics as the deviation from end-of-cycle activity ratios becomes more severe for longer T_c. Finally, the shutdown history is shown to have a very small impact, in agreement with $f(\vec{\beta}, \vec{\gamma}) = 1$ in Sec. III. The maximum errors in percent due to the use of our analytical expressions for the reactor parameters are provided in Tab. I.

	Φ Diagnostics		T_c Diagnostics		
	ϵ	ρ	α_1	α_2	α_3
Φ_t	$\sim 0\%$	$\sim 0\%$	3.86%	0.57%	−3.27%
ϕ_f	0.54%	0.24%	−0.47%	−0.19%	−0.14%
T_c	0%	0%	−0.99%	−0.12%	0.89%
N_s	0%	0%	0.10%	0.01%	−0.10%
T_s	0%	0%	−0.17%	−0.16%	−0.14%
Overall	±0.54%	±0.24%	±4.02%	±0.63%	±3.40%

TABLE I. Analytical errors for the fluence (^{235}U/^{238}U and ^{236}U/^{235}U ratios) and cooling time ($\alpha_1 = {}^{137}$Cs/^{155}Eu, $\alpha_2 = {}^{137}$Cs/^{125}Sb, and $\alpha_3 = {}^{155}$Eu/^{125}Sb ratios) diagnostics given by Eq. 2 and Eq. 9. Each cell shows the maximum expected error over a particular reactor parameter (the thermal fluence Φ_t, fast flux ϕ_f, cooling time T_c, number of shutdowns N_s, and length of shutdowns T_s) range. The overall error for each diagnostics is the individual errors summed in quadrature, which provides a conservative maximum.

Overall, from Tab. I, one can see that the diagnostics derived in Eq. 2 for the fluence have extremely small errors and one can expect the correct fluence within $\sim 0.5\%$. For the cooling time diagnostic in Eq. 9, the errors are more substantial as the fragment systems are more complex. Overall, our diagnostics return the correct cooling time within $\sim 4\%$, $\sim 0.6\%$, and $\sim 3.4\%$ for the ^{137}Cs/^{155}Eu, ^{137}Cs/^{125}Sb, and ^{155}Eu/^{125}Sb ratios, respectively. The linear-averaging in Sec. III returned the lowest errors, but ignores the quadratic behavior of ^{239}Pu at low burnup. We verified that the errors in Tab. I can be effectively eliminated when we account for the non-linear nature of ^{239}Pu at low burnups and calculate Eq. 9 to $\mathcal{O}((\tilde{\lambda} T_{\text{irr}})^2)$. We note that these errors are strictly from the analytical expressions and contain no systematic errors, such as fractionation or experimental uncertainties. We have also calculated the expected

^{239}Pu abundance using a similar analytical method with errors of $\sim 0.25\%$, but this calculation requires knowledge of both ϕ and $T_{\rm irr}$, so we have excluded it from our analysis. The theory errors of Tab. I are lower than the experimental measurement errors. With these notes in mind, we use these diagnostics to determine the thermal fluence and extract information about systematic errors from three cooling time diagnostics.

V. EXPERIMENTAL APPLICATION

Ten archived samples were analyzed for their U and Pu isotopics, as well as the activities of several fission fragments. The actinides were separated and measured as described in Ref. [14]. In short, U metal or UO_3 samples are dissolved in HNO_3, then loaded and separated on anion exchange columns to achieve separation of Pu from U. Isotope ratios and isotope dilution measurements were determined by TIMS. Fission fragments were measured by gamma spectrometry [15]. Samples H and K were in UO_3 form, while the remainder were uranium metal.

Both fluence diagnostic methods were attempted, but discrepancies were observed between the $^{236/235}$U and $^{235/238}$U ratios in very low burnup cases as shown in Fig. 3. The fluences determined in samples D through

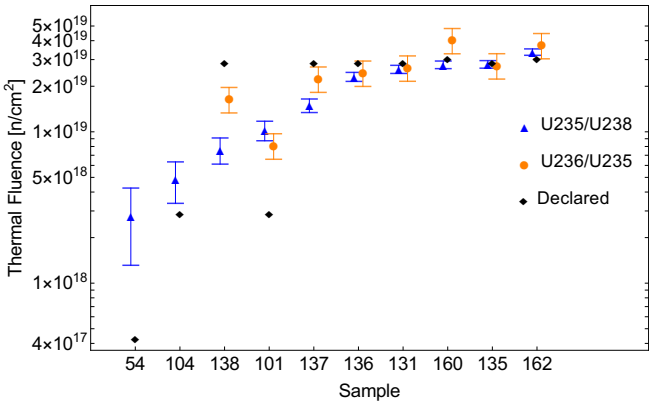

FIG. 3. The derived thermal fluence via the $^{235/238}$U (triangles) or $^{236/235}$U (circles) ratios compared with the declared values (diamonds). Both methods are self-consistent and in good agreement with the declared values in higher fluence samples. The $^{236/235}$U diagnostic could not be used in samples with trace ^{236}U amounts. Errors are the 1σ experimental and theoretical errors summed in quadrature.

K were all nearly self-consistent. Sample C reported fluences that deviate more strongly. Samples A and B were contaminated with ^{236}U memory effects, so their values were not used. The chemical analyses of the remaining samples were conducted at a later time, correcting the ^{236}U issue. Overall, it appears that our method of extracting the thermal fluence via Eq. 2 is accurate and self-consistent for the majority of samples with $\Phi \geq 10^{19}$ n/cm^2. Below this limit, the low concentrations of ^{236}U created experimental difficulties in acquiring the fluence with multiple methods. Thus, one can determine the thermal fluence with two independent diagnostics in samples with appreciable amounts of ^{236}U, but must rely solely on the $^{235/238}$U ratio in extremely low-burnup samples with trace levels of ^{236}U. The ϵ diagnostic is only valid when ϵ_0 is known, so the ρ diagnostic should be used if enough ^{236}U is present. The average difference between the two diagnostics was 19.9%.

In determining the total cooling time, we used the ratios identified in Sec. IV. Figure 4 illustrates the agreement and tension between the different diagnostics. A few samples performed relatively well, but most demonstrated disagreement between the three cooling time diagnostics. In particular, the ^{155}Eu-based determinations

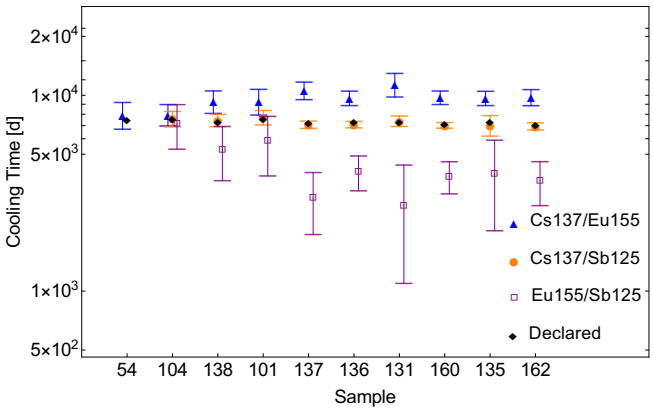

FIG. 4. The derived cooling times via the α_1 (triangles), α_2 (circles), and α_3 (open squares) diagnostics compared with the declared values (diamonds). See text for α definitions. The disagreement between the diagnostics indicates the presence of systematic errors, such as an initial europium abundance or fractionation. Errors are the 1σ experimental and theoretical errors summed in quadrature.

of T_c showed disagreement with the ^{137}Cs/^{125}Sb ratio as the inferred fluence rises. Leakage of volatile fission fragments, such as ^{85}Kr, can occur at the $\gtrsim 13\%$ level in PWR fuels [35] so these ratios were removed. A portion of the bias from ^{155}Eu-based diagnostics can be explained by the over-estimation of the ^{239}Pu-component when linearly averaging $\vec{\Sigma}_{\rm fiss}$ and the need to compute T_c to second order, but these errors will only approach the $3-4\%$ level. We note that fission fragments that have very different yields for each fissile, such as ^{155}Eu, will be more dramatically affected by this linear averaging. In our specific case, the natural uranium fuel and very low burnup remove this concern as the ^{239}Pu fission rate and abundance are orders of magnitude below that of ^{235}U. One can calculate the necessary increase in ^{155}Eu activity to bring all three diagnostics into agreement. These values vary from $\sim 10\%$ to about a factor of 3. Samples with higher fluences required larger ^{155}Eu increases, as would be expected in the case of fractionation. The average error between the ^{137}Cs/^{125}Sb diagnostic and the declared cooling times was 2% for samples B through K. The ^{125}Sb

abundance was not measured in sample A. The average diagnostic discrepancy was found to be $\sim 37\%$ between the ^{155}Eu-based diagnostics and the ^{137}Cs/^{125}Sb ratio. We note that the use of multiple T_c diagnostics allows one to detect the presence of systematic errors, such as the fractionation of ^{155}Eu, and identify the best nuclides to use as diagnostic tags. This technique must be used in the very low burnup regime as traditional same-species ratios are impractical.

VI. CONCLUSION

The work conducted here demonstrates that the thermal fluence can be determined in low burnup samples using the ^{235}U/^{238}U and ^{236}U/^{235}U ratios. These ratios are common fluence diagnostics, which were verified with detailed reactor simulations and then experimentally demonstrated to be accurate and self-consistent when enough ^{236}U is produced above the detection threshold. The average discrepancy between the two fluence diagnostics in our low burnup samples was 19.9% for $\Phi > 10^{19}\,\mathrm{n/cm^2/sec}$.

The low burnup of our reactor samples required new cooling time diagnostics to be derived, as the concentrations of standard diagnostic tags are below detection thresholds or long cooling times prohibit their use. The new cooling time diagnostics utilized simple linear fission fragments with long half-lives and considerable fission yields. Four such fragments were identified and the derived diagnostics were verified in low burnup scenarios. The experimentally determined cooling times were shown to be consistent in some samples, but varied by $\sim 37\%$ on average. In addition, leakage of volatile gases invalidated the diagnostics using ^{85}Kr. Overall, the ^{137}Cs/^{125}Sb ratio seemed to agree with the sample age across all samples. Differing results for the cooling time, as measured by severa diagnostics, could be explained by the fractionation of ^{155}Eu with larger sample fluence, even in the very low burnup regime.

The fluence and cooling time derivation should be conducted in tandem, where the Φ determination would be used to derive $\langle\vec{\Sigma}_{\mathrm{fiss}}\rangle_\Phi$ and verify that the sample has a burnup low enough to validate the simple analytical expressions for T_c. This work provides verification of fluence diagnostics and new cooling time diagnostic techniques to determine the presence of systematic errors in low burnup samples, both of which have applications in nonproliferation and verification.

ACKNOWLEDGMENTS

We would like to thank the analytical chemistry team: L. Colletti, E. Lujan, K. Garduno, T. Hahn, L. Walker, A. Lesiak, P. Martinez, F. Stanley, R. Keller, M. Thomas, K. Spencer, L. Townsend, D. Klundt, D. Decker, and D. Martinez. Los Alamos National Laboratory supported this work through LDRD funding.

[1] A. V. Stepanov, T. P. Makarova, B. A. Bibichev, A. M. Fridkin, A. V. Lovtsyus, L. D. Preobrazhenskaya, A. A. Lipovskii, and A. N. Timofeev, "Determination of burnup and isotope composition for spent VVÉR-365 fuel," Soviet Atomic Energy **49**, 673–678 (1980).

[2] Thomas W. Wood, Bruce D. Reid, John L. Smoot, and James L. Fuller, "Establishing confident accounting for Russian weapons plutonium," The Nonproliferation Review **9**, 126–137 (2002), http://dx.doi.org/10.1080/10736700208436898.

[3] Sergei F Boulyga and J Sabine Becker, "Isotopic analysis of uranium and plutonium using ICP-MS and estimation of burn-up of spent uranium in contaminated environmental samples," Journal of Analytical Atomic Spectrometry **17**, 1143–1147 (2002).

[4] Sergei F. Boulyga and Klaus G. Heumann, "Determination of extremely low 236U/238U isotope ratios in environmental samples by sector-field inductively coupled plasma mass spectrometry using high-efficiency sample introduction," Journal of Environmental Radioactivity **88**, 1–10 (2006).

[5] Jung Suk Kim, Young Shin Jeon, Soon Dal Park, Yeong-Keong Ha, and Kyuseok Song, "Analysis of high burnup pressurized water reactor fuel using uranium, plutonium, neodymium, and cesium isotope correlations with burnup," Nuclear Engineering and Technology **47**, 924–933 (2015).

[6] B. D. Reid, W.C. Morgan, E.F. Love Jr, D.C. Gerlach, S.L. Peterson, J.V. Livingston, L.R. Greenwood, and J.P. McNeece, *Graphite Isotope Ratio Method Development Report: Irradiation Test Demonstration of Uranium as a Low Fluence Indicator*, Tech. Rep. (1999).

[7] CJ Gesh, "A Graphite Isotope Ratio Method Primer: A Method for Estimating Plutonium Production in Graphite Moderated Reactors," PNNL-14568, February (2004).

[8] Alex Gasner and Alexander Glaser, "Nuclear Archaeology for Heavy-Water-Moderated Plutonium Production Reactors," Science and Global Security **19**, 223–233 (2011).

[9] S. Caruso, M. Murphy, F. Jatuff, and R. Chawla, "Validation of 134Cs, 137Cs and 154Eu single ratios as burnup monitors for ultra-high burnup {UO2} fuel," Annals of Nuclear Energy **34**, 28–35 (2007).

[10] S.A. Ansari, M. Asif, T. Rashid, and K.G. Qasim, "Burnup studies of spent fuels of varying types and enrichment," Annals of Nuclear Energy **34**, 641–651 (2007).

[11] Klaus Mayer, Maria Wallenius, and Zsolt Varga, "Nuclear Forensic Science: Correlating Measurable Material Parameters to the History of Nuclear Material," Chemical Reviews **113**, 884–900 (2012).

[12] Ian Gauld and Matthew Francis, "Investigation of passive gamma spectroscopy to verify spent nuclear fuel content," (51 Annual Meeting of the Institute of Nuclear Materials Management (INMM), 2010).

[13] A. C. Hayes and Gerard Jungman, "Determining Reactor Flux from Xenon-136 and Cesium-135 in Spent Fuel," Nucl. Instrum. Meth. **A690**, 68–74 (2012), arXiv:1205.6524 [nucl-th].

[14] Benjamin Byerly, Lav Tandon, Anna Hayes-Sterbenz, Patrick Martinez, Russ Keller, Floyd Stanley, Khalil Spencer, Mariam Thomas, Ning Xu, and Michael Schappert, "Determination of initial fuel state and number of reactor shutdowns in archived low-burnup uranium targets," Journal of Radioanalytical and Nuclear Chemistry (2015), 10.1007/s10967-015-4538-y.

[15] Lav Tandon, Kevin Kuhn, Patrick Martinez, Joseph Banar, Laurie Walker, Terry Hahn, David Beddingfield, Donivan Porterfield, Steven Myers, Stephen LaMont, Daniel Schwartz, David Gallimore, Scott Garner, Khalil Spencer, Lisa Townsend, Heather Volz, Russ Gritzo, Rodney McCabe, Ramiro Pereyra, Dominic Peterson, Mark Scott, Christy Ruggiero, Diana Decker, and Amy Wong, "Establishing reactor operations from uranium targets used for the production of plutonium," Journal of Radioanalytical and Nuclear Chemistry **282**, 573–579 (2009).

[16] H. Natsume, H. Umezawa, S. Okazaki, T. Suzuki, T. Sonobe, and S. Usuda, "Sequential Ion-Exchange Separation of Heavy Elements and Selected Fission Products for Burnup Measurement," Journal of Nuclear Science and Technology **9**, 737–742 (1972).

[17] R.M. Abernathey, G.M. Matlack, and J.E. Rein, *Sequential Ion Exchange Separation and Mass Spectrometric Determination of Neodymium, Uranium, and Plutonium in Mixed Oxide Fuels for Burnup and Isotopic Distribution Measurements* (1972).

[18] S.F. Marsh, M.R. Ortiz, and R.M. Abernathey, "Improved two-column ion exchange separation of plutonium, uranium, and neodymium, in mixed uranium-plutonium fuels for burnup measurement," LA-5568 (1974).

[19] A.Martín Sánchez, F.Vera Tomé, J.Díaz Bejarano, and M.Jurado Vargas, "A rapid method for determination of the isotopic composition of uranium samples by alpha spectrometry," Nuclear Instruments and Methods in Physics Research Section A: Accelerators, Spectrometers, Detectors and Associated Equipment **313**, 219–226 (1992).

[20] J.L. Iturbe, " Identification of ^{236}U in commercially available uranium compounds by alpha particle spectrometry," Applied Radiation and Isotopes **43**, 817–818 (1992).

[21] Patrick Huber and Patrick Jaffke, "Neutron capture and the antineutrino yield from nuclear reactors," Phys. Rev. Lett. **116**, 122503 (2016), arXiv:1510.08948 [hep-ph].

[22] E. C. Freiling and M. A. Kay, "Radionuclide Fractionation in Air-Burst Debris," Nature **209**, 236–238 (1966).

[23] J. Navarro, R. Aryaeinejad, and D.W. Nigg, *A Feasibility Study to Determine Cooling Time and Burnup of ATR Fuel Using a Nondestructive Technique and Three Types of Gamma-ray Detectors*, Tech. Rep. (2011).

[24] B. Bergelson, A. Gerasimov, and G. Tikhomirov, "Influence of High Burnup on the Decay Heat Power of Spent Fuel at Long-Term Storage," (2013).

[25] Oak Ridge National Laboratory, *Scale: A Comprehensive Modeling and Simulation Suite for Nuclear Safety Analysis and Design*, Oak Ridge National Laboratory, 6th ed. (2011).

[26] O. Meplan, *MURE, MCNP Utility for Reactor Evolution - User Guide - Version 1.0*, Report: LPSC 0912 (2009).

[27] Maria Pusa and Jaakko Leppänen, "Computing the matrix exponential in burnup calculations," Nuclear Science and Engineering **164**, 140–150 (2010).

[28] H. Bateman, "The solution of a system of differential equations occurring in the theory of radioactive transformations," Proc. Cambridge Philos. Soc. **15**, 423 (1910).

[29] A.E. Isotalo and P.A. Aarnio, "Comparison of depletion algorithms for large systems of nuclides," Annals of Nuclear Energy **38**, 261–268 (2011).

[30] S. Holloway and WB Wilson, "CINDER08: The next generation," in *PSI Proceedings* (2008).

[31] M. B. Chadwick *et al.*, "ENDF/B-VII.1 Nuclear Data for Science and Technology: Cross Sections, Covariances, Fission Product Yields and Decay Data," Nucl. Data Sheets **112**, 2887–2996 (2011).

[32] M. A. Kellett, O. Bersillon, and R. W. Mills, *The JEFF-3.1/-3.1.1 radioactive decay data and fission yields sublibraries* (Nuclear Energy Agency, 2009).

[33] K. Shibata, O. Iwamoto, T. Nakagawa, N. Iwamoto, A. Ichihara, S. Kunieda, S. Chiba, K. Furutaka, N. Otuka, T. Ohsawa, T. Murata, H. Matsunobu, A. Zukeran, S. Kamada, and J. Katakura, "JENDL-4.0: A New Library for Nuclear Science and Engineering," Journal of Nuclear Science and Technology **48**, 1–30 (2011).

[34] Jerzy Cetnar, "General solution of Bateman equations for nuclear transmutations," Annals of Nuclear Energy **33**, 640–645 (2006).

[35] V. Metz, E. Gonzalez-Robles, N. Muller, E. Bohnert, M. Herm, M. Lagos, B. Kienzler, D. Serrano-Purroy, J.Y. Colle, O. Benes, F. Naisse, T. Wiss, R.J.M. Konings, D.H. Wegen, D. Papaioannou, R. Gretter, R. Nasyrow, V.V. Rondinella, J.-P. Glatz, H. Curtius, H.W. Muskes, N. Like, D. Bosbach, I. Gunther-Leopold, E. Curti, A. Froideval Zumbiehl, H.P. Linder, K. Govers, M. Verwerft, W. Van Renterghem, K. Lemmens, T. Mennecart, C. Cachoir, L. Adriaensen, A. Dobney, M. Gysemans, J. Vandenborre, A. Traboulsi, G. Blain, J. Barbet, M. Fattahi, R. Sureda Pastor, E. Slonszki, Z. Hozer, and O. Roth, "Characterisation of spent nuclear fuel samples and description of methodologies and tools to be applied in FIRST-Nuclides," CP-FP7-295722 (2013).